

## Electron-Stimulated Desorption Enhanced by Coherent Scattering

H. Sambe and D. E. Ramaker

*Chemistry Department, George Washington University, Washington, D.C. 20052*

and

L. Parenteau and L. Sanche

*Canadian Medical Research Council Group in Radiation Sciences, Faculty of Medicine, University of Sherbrooke, Sherbrooke, Quebec J1H5N4, Canada*

(Received 8 June 1987)

The electron-stimulated  $O^-$  desorption yields from  $O_2$  condensed on a thick rare-gas (Ar, Kr, or Xe) film are reported. It is shown that coherent scattering of electrons in the rare-gas film dramatically enhances the  $O^-$  yields near the Bragg reflection energies.

PACS numbers: 79.20.Kz, 31.70.Ks, 34.80.Gs, 79.90.+b

We report electron-stimulated  $O^-$  desorption (ESD) yields from  $O_2$  condensed on thick rare-gas (Ar, Kr, or Xe) films previously condensed on a Pt substrate. The  $O^-$  yield from  $O_2$ /Ar/Pt increases by an order of magnitude as the Ar layer thickness increases from 8 to 32 monolayers (ML). We show that this enhancement arises from an indirect process involving coherent electron scattering in the rare-gas (RG) film. We further demonstrate that the  $O^-$  yield via this indirect coherent process is two orders of magnitude greater than that from the direct process near the Bragg reflection (BR) energies. We conclude that this dramatic enhancement of the indirect process arises from the standing-wave character of the electronic wave function near the BR energies.

The ESD  $O^-$  yields from  $O_2$ /RG/Pt are measured as a function of electron energy for  $O_2$  coverages in the range 0.02–1.0 monolayers (ML) and RG thicknesses in the range 1–32 ML. The apparatus has been described previously.<sup>1</sup> The incident angle of the electron beam is  $20^\circ$  from the surface, and the  $O^-$  ions are measured by a quadrupole mass spectrometer positioned at  $70^\circ$  from the surface. The film thicknesses are estimated to within 20% by a method described previously.<sup>2</sup> A rare gas is condensed near its sublimation temperature on a clean Pt ribbon, and the  $O_2$  gas is condensed onto the RG film at 17 K. Electron transmission spectra (ETS) data<sup>3</sup> reveal that the RG films are essentially ordered, since BR minima are observed around 5 and 9 eV for Ar, 4, 7, and 9 eV for Kr, and 2.5, 5, and 7.5 for Xe. In contrast, Xe films prepared well below the sublimation temperature do not exhibit BR minimum in ETS.<sup>4</sup> Data also indicate that the Ar films seem to be more ordered than the Kr and Xe films.<sup>5</sup>

Figure 1 shows the ESD  $O^-$  yields from  $O_2$  (0.1 ML)/Ar(1–32 ML)/Pt as a function of incident electron energy. As the Ar thickness increases, the three features at 6, 18, and 24 eV grow faster than the remainder of the spectrum, and at large thicknesses ( $> 20$  ML) dom-

inate the spectrum. The  $O^-$  yields at these three energies are plotted as a function of the Ar thickness in Fig. 2. Similarly prepared  $O_2$ /Kr/Pt samples give qualitatively similar results, but with the following quantitative differences. The 6-eV feature for Ar is narrower than

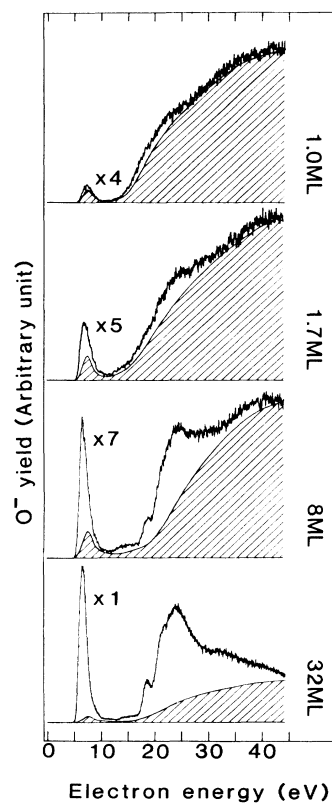


FIG. 1. Comparison of the ESD  $O^-$  yield curves obtained from  $O_2$ /Ar/Pt with a constant (0.1 ML)  $O_2$  coverage and variable (1–32 ML) Ar thicknesses. The shaded areas indicate our estimated contributions due to the direct process.

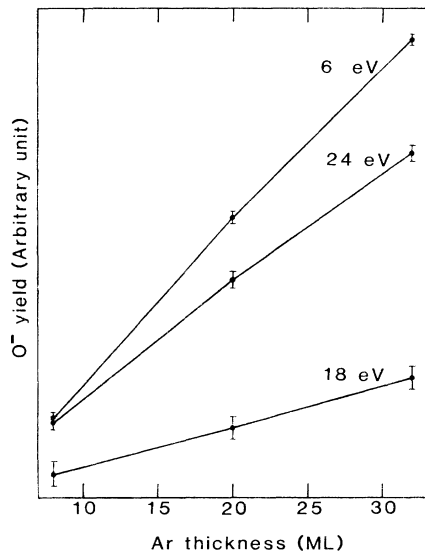


FIG. 2. Ar thickness dependence of the ESD  $O^-$  yields from  $O_2(0.1 \text{ ML})/\text{Ar}/\text{Pt}$ . The incident electron energies are as indicated.

that for Kr (Fig. 3). The rate of increase in the  $O^-$  yield with RG layer thickness (i.e., the slope in Fig. 2) is 3 times larger for Ar than for Kr. The separation of the first two features are 12.2 eV for Ar, but only 10.5 eV for Kr.

The spectral shape of the 6-eV feature depends on the RG, the thickness and structural order of the RG layer, and the  $O_2$  coverage. It is broad and symmetric at small RG thicknesses, but sharp, asymmetric, and shifted to lower energy at larger thicknesses (Fig. 1). It is much narrower at smaller  $O_2$  coverages (solid curves in Fig. 3) than at larger coverages (dotted curves in Fig. 3). The dependence on the RG can be seen in Fig. 3, and on the structural order of the RG in Fig. 4.

The experimental results described above can be explained in terms of three processes which we call the direct (D), elastic-indirect (EID), and inelastic-indirect (IID) processes. In the D process, an incident electron collides with an  $O_2$  on the surface and produces an  $O^-$  directly. In the EID process, an incident electron at an energy below the first electronic-excitation energy (first  $E_{ex}$ ) of the RG, passes through the  $O_2$  layer without loss of energy, undergoes quasielastic multiple scattering in the RG, and returns to the surface, where it collides with an  $O_2$  and produces  $O^-$  as in the D process. The IID process is identical to the EID, except that the electron upon initial entry into the RG film, suffers loss of energy by electronically exciting the RG. At electron energies above the first  $E_{ex}$ , the inelastic mean free path in RG films is very short ( $\approx 10 \text{ \AA}$ ).<sup>7</sup>

The  $O^-$  yields via these processes are proportional to

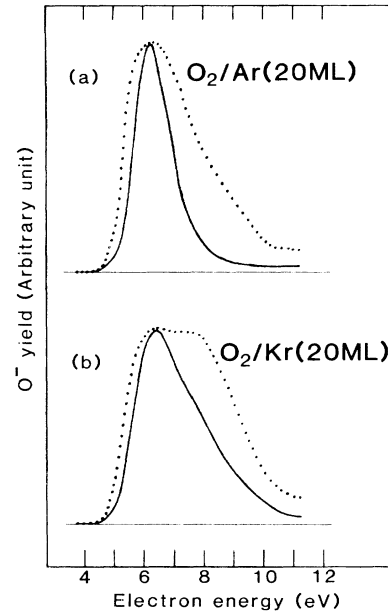


FIG. 3. Comparison of the ESD  $O^-$  yield curves obtained with a constant rare-gas (Ar or Kr) thickness (20 ML) but with different  $O_2$  coverages, 0.03 ML (solid curves) and 1.0 ML (dotted curves).

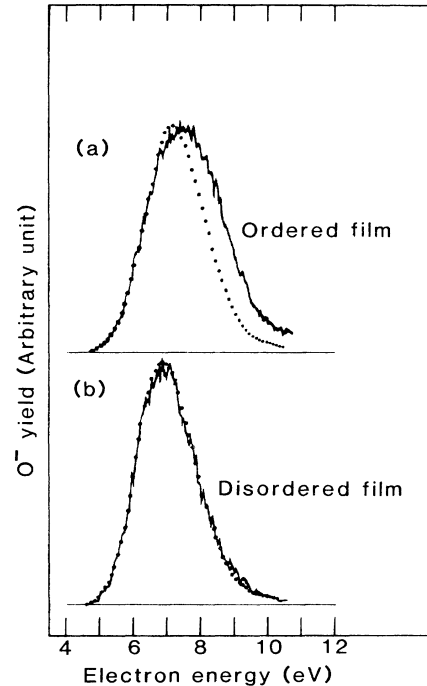


FIG. 4. ESD  $O^-$  yield curves obtained from  $O_2(0.1 \text{ ML})/\text{Xe}(20 \text{ ML})/\text{Pt}$  prepared at 40 K (top) and 17 K (bottom). Also shown are ESD  $O^-$  yield curves from  $O_2$  gas (dotted curves) (from Ref. 6).

the following expressions:

$$\begin{aligned} D &\propto \Theta \sigma(E), \quad \text{EID} \propto [1 - \Theta \sigma_{\text{BI}}(E)] P_{\text{B}}(\text{RG}, \tau, E) \Theta \sigma(E), \\ \text{IID} &\propto [1 - \Theta \sigma_{\text{BI}}(E)] P_{\text{ex}}(\text{RG}, E_{\text{ex}}, E) P_{\text{B}}(\text{RG}, \tau, E - E_{\text{ex}}) \Theta \sigma(E - E_{\text{ex}}). \end{aligned} \quad (1)$$

Here,  $E$  denotes the incident electron energy,  $\Theta$  the  $\text{O}_2$  coverage, and  $\sigma(E)$  the  $\text{O}^-$  yield cross section from  $\text{O}_2$  on the RG film.  $\sigma(E)$  is assumed to be independent of the RG thickness beyond 7 ML, because the effects of neutralization and the image-charge force due to the PT substrate die out rapidly with film thickness, and the effects of polarization due to the RG become constant with film thickness. The factor  $[1 - \Theta \sigma_{\text{BI}}(E)]$  gives the probability of passing through the  $\text{O}_2$  layer with loss of energy, where  $\sigma_{\text{BI}}(E)$  is equal to a sum of the elastic backscattering and the total inelastic cross sections of  $\text{O}_2$ . Because of this factor, the EID and IID contributions should decrease relative to the D contribution with increasing  $\text{O}_2$  coverage.  $P_{\text{B}}(\text{RG}, \tau, E)$  denotes the probability of the electron returning to the surface, which depends on the RG, the RG thickness ( $\tau$ ), and the electron energy in the film.  $P_{\text{ex}}(\text{RG}, E_{\text{ex}}, E)$  denotes the electronic-excitation probability of the RG film by electron impact at energy  $E$ . Since  $\sigma_{\text{BI}}(E)$  and  $P_{\text{ex}}(E)$  are slowly varying functions of  $E$ ,<sup>8</sup> the  $E$  dependence of the D, EID, and IID contributions are primarily determined by  $\sigma(E)$  and  $P_{\text{B}}(E)$ . Because of the short inelastic mean free path, the  $\text{O}^-$  yield,  $Y(\text{RG}, t, E)$ , below and above the first  $E_{\text{ex}}$  are given by  $Y = \text{D} + \text{EID}$  and  $Y = \text{D} + \text{IID}$ , respectively.

Figure 2 shows that the  $\text{O}^-$  yields at 6, 18, and 24 eV all increase as the Ar layer thickness increases. Equation (1) indicates that this relationship exists because of the two indirect processes. The data provide two other criteria to verify our model; if Eq. (1) is true, (i) the peak-to-peak energy difference between the EID and IID features should be equal to one of the  $E_{\text{ex}}$  of the RG film, and (ii) the relative intensities of these EID and IID features at  $E_p$  and  $E_p + E_{\text{ex}}$  should satisfy the relation

$$\begin{aligned} \frac{Y(E_p + E_{\text{ex}}, \tau) - Y(E_p + E_{\text{ex}}, \tau')}{Y(E_p, \tau) - Y(E_p, \tau')} \\ = \text{constant with thickness,} \quad (2) \end{aligned}$$

where  $\tau$  and  $\tau'$  are two different RG thicknesses. The 6- and 18-eV features in Fig. 1 satisfy both criteria. Their peak-to-peak energy separation ( $12.2 \pm 0.1$  eV) agrees with the lowest two  $E_{\text{ex}}$  (12.1 and 12.2 eV) of solid Ar.<sup>9</sup> Evaluation of Eq. (2) by use of the 8- and 20-ML data gives 0.24, and by use of the 20- and 32-ML data gives 0.28. The 6- and 24-eV features satisfy the intensity criterion [0.71 vs 0.70 in Eq. (2)]; however, the energy criterion cannot be demonstrated because experimental constant-final-state (CFS) energy-loss spectra are not available. CFS spectra are required in this case because the 24-eV feature corresponds to excitation in the Ar

continuum. The above analysis verifies Eq. (1) and also establishes that the 6-, 18-, and 24-eV features observed for  $\text{O}_2(0.1 \text{ ML})/\text{Ar}(32 \text{ ML})$  arise predominately from the EID, IID, and IID processes, respectively. Similar analysis for  $\text{O}_2/\text{Kr}$  shows that the peak around 6.5 eV for  $\text{O}_2(0.03 \text{ ML})/\text{Kr}(20 \text{ ML})$  is dominated by the EID process, but that around 8 eV for  $\text{O}_2(1.0 \text{ ML})/\text{Kr}(20 \text{ ML})$  is dominated by the D process.

Satisfaction of Eq. (2) confirms our previous assumption that  $\sigma(E)$  should be independent of the RG thickness beyond 7 ML. The spectral shape of  $\sigma(E)$ , or the D contribution, is expected to be similar to the  $\text{O}^-$  yield from  $\text{O}_2$  gas, except for the relative magnitude of the contributions below 10 eV and above 17 eV. Below 10 eV, the  $\text{O}^-$  arises through a charged  $\text{O}_2^-$  intermediate [via the dissociative attachment (DA) process]; but above 17 eV, through a neutral  $\text{O}_2^*$  intermediate [via the dipolar dissociation (DD) process]. Polarization of the thick RG layer reduces the  $\text{O}^-$  yield via the DA process, but enhances that via the DD process, compared with that for  $\text{O}_2$  gas.<sup>10</sup> Our estimates of the D contribution, indicated in Fig. 1 by the shaded areas, are based on the above considerations. The intensity ratio  $\text{EID}/\text{D} = [1 - \Theta \sigma_{\text{BI}}] P_{\text{B}}$  for  $\text{O}_2(0.1 \text{ ML})/\text{Ar}(32 \text{ ML})$  is about 70 at the peak energy of the 6-eV feature, which is about 1 eV lower than the peak energy of the D contribution. Assuming that  $[1 - \Theta \sigma_{\text{BI}}]$  for  $\Theta = 0.1$  is about 0.8, we estimate that  $P_{\text{B}}$  is around 90. For thicker and more ordered Ar films, we expect even larger values of  $P_{\text{B}}$ . Since the maximum  $P_{\text{B}}$  obtainable by incoherent multiple scattering is around 2, coherent scattering must be playing a dominant role.

The spectral shape of the 6-eV feature for the different RG films can be correlated with the BR minima observed in ETS data. The 6-eV line shape from a disordered Xe film is virtually identical with that from  $\text{O}_2$  gas [Fig. 4(b)]. Since  $\sigma(E)$  is virtually identical in the 5–10-eV range with that from  $\text{O}_2$  gas,  $P_{\text{B}}(E)$  for the disordered film must be nearly invariant with  $E$  over this same energy range. However,  $P_{\text{B}}(E)$  for the ordered film must vary over this energy range, since the line shape of the ordered Xe film differs from that for  $\text{O}_2$  gas [Fig. 4(a)]. The 6-eV line shape for Ar depends on the  $\text{O}_2$  coverage [Fig. 3(a)], and at the lower coverage (0.03 ML), it is narrower than  $\sigma(E)$  [Fig. 3(a), solid curve] and its peak is shifted to lower energy (Figs. 1 and 3). All these suggest that  $P_{\text{B}}(E)$  for Ar is strongly enhanced near the first BR minimum around 5 eV. The peak for Kr at the lower  $\text{O}_2$  coverage is also shifted to lower energy [Fig. 3(b)]; however, the line shape is wider than  $\sigma(E)$  apparently because two BR energies (4 and 7 eV)

partially overlap with  $\sigma(E)$ . The  $O^-$  yield is enhanced for Ar more strongly than for Kr, because the first BR minimum for Ar is closer to the peak of  $\sigma(E)$ , and perhaps also because the Ar film is more ordered. This analysis indicates that  $P_B(E)$  is enhanced near BR energies, especially strongly near the first BR minimum.

It is well known that for a perfect crystal the electronic wave functions just above and below the energy band gaps, which arise from the BR's, have standing-wave character.<sup>11</sup> We conclude that this standing-wave character is responsible for the large enhancement of  $P_B$  near the BR energies. The increase of  $P_B$  with RG thickness is also consistent with this since the standing-wave character should increase with RG thickness. However, this raises an interesting question. How does a relatively small increase in the amplitude of the electronic wave function (i.e., at most a factor of 2 due to the standing-wave character) cause such a dramatic increase in the  $O^-$  desorption yield (a factor of  $10^2$ )?

Two of us (H.S. and D.E.R.) acknowledge partial sup-

port from the U.S. Office of Naval Research.

---

<sup>1</sup>L. Sanche and L. Parenteau, *J. Vac. Sci. Technol. A* **4**, 1240 (1986).

<sup>2</sup>L. Sanche, *J. Chem. Phys.* **71**, 4860 (1979); E. Keszei *et al.*, *J. Chem. Phys.* **85**, 7396 (1986).

<sup>3</sup>G. Bader *et al.*, *Phys. Rev. B* **30**, 78 (1984).

<sup>4</sup>G. Bader *et al.*, *Phys. Rev. B* **26**, 6019 (1982).

<sup>5</sup>G. Perluzzo *et al.*, *Phys. Rev. Lett.* **55**, 545 (1985).

<sup>6</sup>D. Rapp and D. D. Briglia, *J. Chem. Phys.* **43**, 1480 (1965).

<sup>7</sup>N. Schwentner *et al.*, *Electronic Excitations in Condensed Rare Gases* (Springer-Verlag, Berlin, 1985), Sec. 7.

<sup>8</sup>S. Trajmar *et al.*, *Phys. Rep.* **97**, 219 (1983).

<sup>9</sup>V. Saile *et al.*, *Extended Abstracts, Fifth International Conference on Vacuum Ultraviolet Radiation Physics*, edited by M. C. Castex, M. Pouey, and N. Pouey (Centre National de la Recherche Scientifique, Meudon, 1977), Vol. 1, p. 79.

<sup>10</sup>H. Sambe *et al.*, to be published.

<sup>11</sup>C. Kittel, *Introduction to Solid State Physics* (Wiley, New York, 1986), 6th ed., Chap. 7.